



# Dimeric $\gamma$ -AApeptides With Potent and Selective Antibacterial Activity

Minghui Wang<sup>1</sup>, Ruixuan Gao<sup>1</sup>, Peng Sang<sup>1</sup>, Timothy Odom<sup>1</sup>, Mengmeng Zheng<sup>1</sup>, Yan Shi<sup>1</sup>, Hai Xu<sup>2</sup>, Chuanhai Cao<sup>3</sup> and Jianfeng Cai<sup>1\*</sup>

<sup>1</sup> Department of Chemistry, University of South Florida, Tampa, FL, United States, <sup>2</sup> College of Chemistry and Chemical Engineering, Central South University, Changsha, China, <sup>3</sup> College of Pharmacy, University of South Florida, Tampa, FL, United States

Over the past few decades, the emergence of antibiotic resistance developed by life-threatening bacteria has become increasingly prevalent. Thus, there is an urgent demand to develop novel antibiotics capable of mitigating this trend. Herein, we report a series of dimeric  $\gamma$ -AApeptide derivatives as potential antibiotic agents with limited toxicity and excellent selectivity against Gram-positive strains. Among them, compound **2** was identified to have the best MICs without inducing drug resistance, even after exposure to MRSA for 20 passages. Time-kill kinetics and mechanistic studies suggested that **2** could mimic host-defense peptides (HDPs) and rapidly eradicate MRSA within 2 hours through disturbing the bacteria membrane. Meanwhile, biofilm formation was successfully inhibited even at a low concentration. Taken together, these results suggested the great potential of dimeric  $\gamma$ -AApeptide derivatives as antibacterial agents.

## OPEN ACCESS

### Edited by:

Tara Louise Pukala,  
University of Adelaide, Australia

### Reviewed by:

Lakshminarayanan Rajamani,  
Singapore Eye Research Institute  
(SERI), Singapore  
Shouguang Jin,  
University of Florida, United States

### \*Correspondence:

Jianfeng Cai  
jianfengcai@usf.edu

### Specialty section:

This article was submitted to  
Medicinal and Pharmaceutical  
Chemistry,  
a section of the journal  
Frontiers in Chemistry

Received: 26 March 2020

Accepted: 27 April 2020

Published: 12 June 2020

### Citation:

Wang M, Gao R, Sang P, Odom T,  
Zheng M, Shi Y, Xu H, Cao C and  
Cai J (2020) Dimeric  $\gamma$ -AApeptides  
With Potent and Selective Antibacterial  
Activity. *Front. Chem.* 8:441.  
doi: 10.3389/fchem.2020.00441

**Keywords:** host defense peptide,  $\gamma$ -AApeptides, antimicrobial, Gram-positive strains, drug resistance

## INTRODUCTION

The emergent antibiotic resistance has already limited the use of many antibiotics and has posed a great threat to public health (Shi et al., 2019a). In the United States, 2 million people get infected by antibiotic-resistant infections every year, which is estimated to cause more than 700,000 deaths (Nimmagadda et al., 2017; Wang et al., 2019). Over the last century Gram-positive bacteria, especially the notorious methicillin-resistant *Staphylococcus aureus* (MRSA), *Staphylococcus epidermidis* (MRSE), and *vancomycin-resistant E. faecal* (VRE), have spread easily and are now becoming the leading cause of bacterial infections within both health-care and community settings (Lee et al., 2018; Niu et al., 2018).

Considerable efforts have been extended to meet the urgent medical needs whereas the antibacterial drug discovery is experiencing a marked decrease (Payne et al., 2006). As an alternative strategy, host defense peptides (HDPs), also termed “antimicrobial peptides (AMPs),” are serving as a first-line defense against bacterial infections in eukaryotic organisms. (Méndez-Samperio, 2014; Teyssières et al., 2016) Previous reports have shown that HDPs, such as indolicidin (Galdiero et al., 2016) and human defensin 5 (Lei et al., 2018), are potential antibiotics based on their membrane disruption (permeabilization and lysis) ability. Unlike conventional antibiotics targeting some specific intracellular and cell wall targets, the main driving force in the selectivity is the electrostatic interaction between HDPs and bacterial membrane (Su et al., 2017; Niu et al., 2018). It is well known that the membrane of bacteria is negatively charged due to the presence of phosphatidylglycerol (PG), whereas mammalian cell membrane consists of zwitterionic sphingomyelin and phosphatidylcholine (PC). In addition, negatively charged lipopolysaccharides

(LPS) and lipoteichoic acids (LTA) on the bacterial membrane further contribute to the selectivity of cationic HDPs for their recognition of bacteria cells (Teng et al., 2016a; Nimmagadda et al., 2017; Su et al., 2017; Niu et al., 2018). After initial selective contact with bacteria, lipophilic side chains of amphipathic HDPs could insert into the lipid bilayer to compromise the membrane stability and integrity through multiple modes, leading to eventual bacterial death (Niu et al., 2018). As the interaction is without the use of a specific protein or DNA targets, this mechanism could explain why HDPs have a low propensity to develop drug resistance, at least partially.

Although these advantages are promising, there are several drawbacks hindering HDPs to advance into clinical settings, including low effectiveness, high toxicity, and difficulty during the synthesis.<sup>12</sup> Recently, peptidomimetics that mimic HDPs have been developed in order to overcome the hurdles, such as  $\alpha/\beta$ -peptides (Karlsson et al., 2006, 2010; Molchanova et al., 2017),  $\alpha/\beta$ -peptoids (Chongsiriwatana et al., 2008, 2011), AApeptides (Shi et al., 2016; Teng et al., 2017b; Li et al., 2018), arylamide oligomers (Hua et al., 2010), and oligoacyllysines (Rotem et al., 2010).  $\gamma$ -AApeptides (oligomers of  $\gamma$ -substituted-N-acylated-N-aminoethyl amino acids), which have shown promising antimicrobial application, were developed based on the  $\gamma$ -PNA backbone (Teng et al., 2017a, 2018, 2019; She et al., 2018; Shi et al., 2019b). One of the most attractive advantages of  $\gamma$ -AApeptides is that the secondary amines on the backbone could be modified and thereby provide opportunities to introduce a wide variety of functional side chains. This could include the introduction of hydrophobic groups and cationic groups that can help mimic the HDPs (Hu et al., 2012; Wu et al., 2012; Li et al., 2014b; Teng et al., 2016b). Other advantages of  $\gamma$ -AApeptides are their higher bioavailability, resistance to proteolytic degradation, and the added benefit that they are easy to synthesize. We recently reported a series of antibacterial agents that are based on  $\gamma$ -AApeptides, which displayed good antibacterial activity (against both Gram-positive and Gram-negative bacteria) (Li et al., 2014a; Padhee et al., 2015; Teng et al., 2016a). Herein, we attempted to utilize a dimerization strategy while developing novel amphiphilic antibiotics based on small sized  $\gamma$ -AApeptides.

## RESULTS AND DISCUSSION

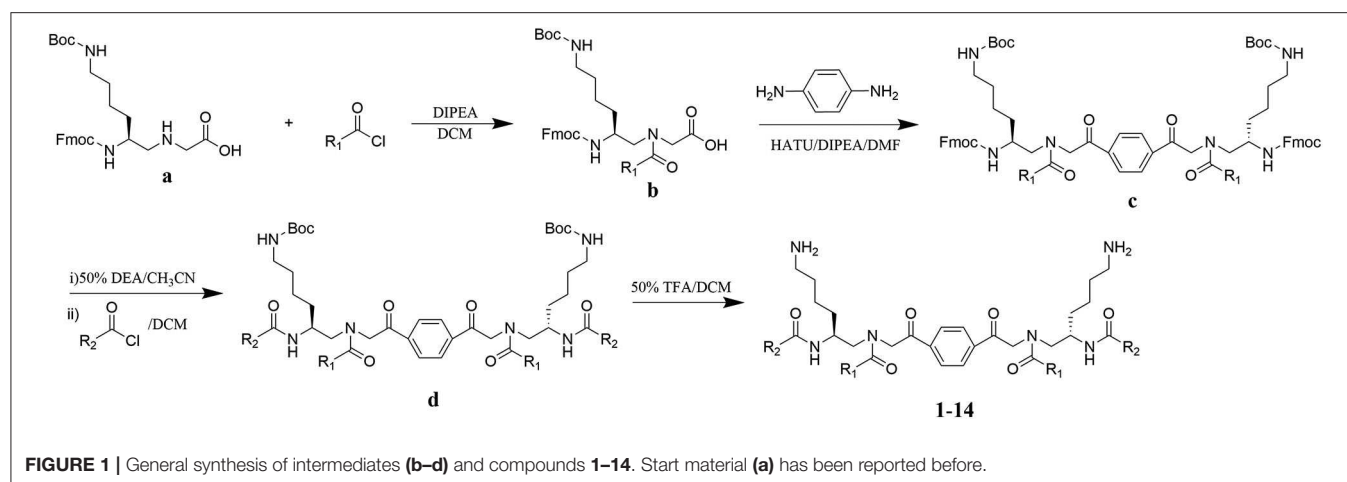
### Design and Synthesis of Dimeric AApeptides

The design of dimeric AApeptides is a very straightforward concept through the use of solid phase peptide chemistry. In order to mimic an amphipathic HDPs bearing both a cationic and hydrophobic group, we prepared lysine-derived AApeptide building blocks containing variable hydrophobic side chains ( $R_1$ ) (**Figure 1b**) (Teng et al., 2016a; Su et al., 2017; Niu et al., 2018). Following that, a *p*-phenylenediamine was used as a linker to dimerize two building blocks (**b**) (Becker et al., 2001; Debnath et al., 2012; Ghosh and Brindisi, 2015). The effort led to a series of dimeric AApeptides after

removal of the Fmoc groups, followed by capping with  $R_2$  tails and final TFA deprotection. Some structures without  $R_2$  tails were also synthesized to evaluate the relationship between the antibacterial activity and the number of cationic groups. We believe the straightforward synthesis of these AApeptides could enhance their potential as practical antibiotic agents.

### *In vitro* Minimum Inhibitory Concentration (MIC) Test and Hemolytic Assay

Having obtained all compounds, their antibacterial efficacy was subsequently evaluated by measuring the minimum inhibitory concentration (MIC). Three significant resistant bacteria, including methicillin-resistant *Staphylococcus aureus* (MRSA) (ATCC 33591), *Staphylococcus epidermidis* (MRSE) (RP62A), and *vancomycin-resistant E. faecalis* (VRE) (ATCC 700802), were chosen for our studies. Meanwhile, hemolytic activity ( $HC_{50}$ ) was also measured to assess the selectivity of these compounds toward bacteria and blood cells. To our delight, most of these compounds showed strong activity against all tested strains. As shown in **Table 1**, the most potent compound **2** exhibited MICs less than  $10\ \mu\text{g}/\text{mL}$  toward all evaluated bacteria, and the activity against MRSA is only  $2\ \mu\text{g}/\text{mL}$ . Importantly,  $HC_{50}$  of almost all compounds are equal or more than  $250\ \mu\text{g}/\text{mL}$ . This indicated that all active compounds are highly selective toward Gram-positive bacteria. The compounds also displayed decent structure activity relationship as expected. **2** and **3** showed excellent activity against both MRSA and MRSE while **2** has a twofold-lower MIC toward VRE. This result indicated that alkyl tails with 10 or 12 carbons were effective to eradicate bacteria cells. Interestingly, with the length of the alkyl tail increased to 14 and 16, compounds **4** and **5** showed activities against all strains over  $25\ \mu\text{g}/\text{mL}$ . This is consistent with our previous findings that significant hydrophobicity, particularly two long alkyl tails, could form hydrophobic clusters that prevent the formation of amphipathic structures necessary for antimicrobial activity (Li et al., 2014b; Singh et al., 2018). By contrast, decreasing carbon tails to 6 (compound **1**) greatly improved the activity against MRSE to  $0.75\ \mu\text{g}/\text{mL}$ , while losing the effectiveness toward MRSA. MICs of **10–14** unveiled that proper bulky hydrophobic groups were beneficial in the design of bactericide. These five compounds have the same (3*r*,5*r*,7*r*)-1-methyladamantane side chain but different tails, including C9, as well as C11 alkyl chain, ethylbenzene, and (3*r*,5*r*,7*r*)-1-methyladamantane. Among them, **10**, which had no tail, was the best toward MRSA and MRSE, with the MICs of  $5\ \mu\text{g}/\text{mL}$  and  $2\ \mu\text{g}/\text{mL}$  respectively. Interestingly, **11** and **14**, which had long fatty chains, did not show activity against any of bacterial strains tested up to  $25\ \mu\text{g}/\text{mL}$ , while **12** and **13** with bulky tails showed much better activity against all three strains. Compounds **7** and **8** also shared a similar trend. It appears that compounds with bulky groups have better activity, due to the larger molecular volume or shorter molecular length of these bulky groups. Therefore, the selection of proper hydrophobic bulky groups when designing HDP-mimicking agents is considerably crucial (Wu et al., 2012; Teng et al., 2016a).



### Bactericidal Time-Kill Kinetics

To evaluate the action mode of our synthetic antibacterial agents, the kinetics of MRSA killing were conducted for the most potent compound **2** at the concentrations of 6  $\mu\text{g/mL}$ , 12  $\mu\text{g/mL}$ , and 24  $\mu\text{g/mL}$  respectively. As shown in **Figure 2**, at the concentrations of 12  $\mu\text{g/mL}$  and 24  $\mu\text{g/mL}$ , all bacteria could be eradicated within 120 mins. Although there were still colonies after 120 mins with treatment of **2** at the 6  $\mu\text{g/mL}$ , the growth of bacteria had an obvious decreasing trend, which indicated that bacteria may all have been eradicated after a longer treatment. The data indicate that compound **2** could eradicate MRSA rapidly.

### Bacteria Membrane Depolarization

HDPs are known to act on the bacterial membrane. As the mimics of HDPs, compounds **1–14** were also expected to kill bacteria through disintegrating the bacterial cell membrane. To this end, 3, 3'- Dipropylthiadicarbocyanine iodide [DiSC3(5)] was used as a fluorogenic probe to detect and measure changes in transmembrane potential. Briefly, fluorescence intensity is very weak when it accumulates on hyperpolarized membranes due to their self-quenching (Niu et al., 2018). However, as long as the integrity of the membrane is interrupted, the fluorescence intensity would increase significantly. This method was used to initially determine the bacterial membrane permeability caused by the compound **2**. As shown in **Figure 3**, the fluorescence intensity has no big difference between two groups within 30 mins. However, after the treatment of MRSA with compound **2**, the fluorescence intensity increased dramatically, whereas the negative control had no big difference. The result suggested that compound **2** disintegrated the MRSA cell membrane, which is the typical antibacterial mode of HDPs.

### Fluorescence Microscopy

Experiments of fluorescent microscopy is also a broadly used method to determine the integrity of bacteria membrane. Propidium iodide (PI) and 4',6-diamidino-2-henylindole (DAPI) are commercially available dyes that stain dead or injured cells with compromised membrane and all cells irrespective of their

viability, respectively. The efficacy of compound **2** to interrupt the bacterial membrane was evaluated by these two dyes. As shown in **Figure 4**, after being stained by DAPI and PI respectively, MRSA negative control only has a bright blue fluorescent in the DAPI channel, which demonstrated that only DAPI was stained on bacterial membrane, suggesting the membrane was intact. When MRSA was treated with compound **2** at the concentration of 6  $\mu\text{g/mL}$  for 2 h, fluorescence could be detected in both channels, indicating that the membrane of MRSA was interrupted after the treatment of **2**.

### TEM Study

Transmission electron microscopy (TEM) is a straightforward method to visualize the interruptive effect of compounds on the membrane of bacteria. Mid log phase MRSA without the treatment of compound **2** had intact membrane (**Figure 5A**). After incubation with **2** at the concentration of 6  $\mu\text{g/mL}$  for 2 h, large amount of cell debris can be detected, demonstrating that the membrane was disintegrated (**Figure 5B**).

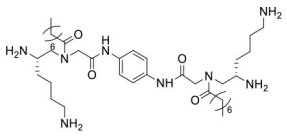
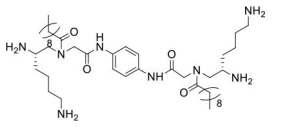
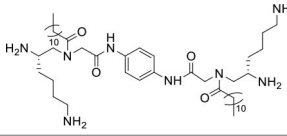
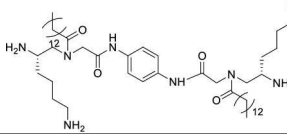
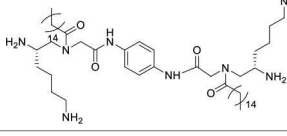
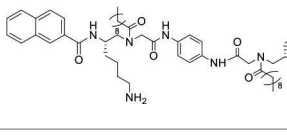
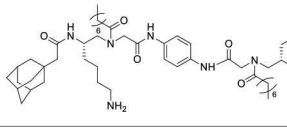
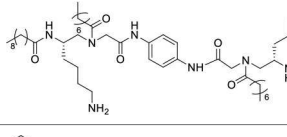
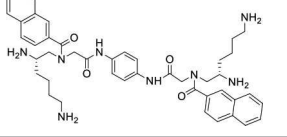
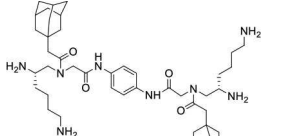
### Bacteria Resistance Study

Drug resistance has already been recognized as one of the fastest growing threats all over the world. As such, a bacteria resistance study was carried out to detect whether the most potent compound **2** could be a prospective compound to overcome the issue. The MIC of compound **2** was determined daily, and then the bacteria suspension with half of the MIC was diluted to  $10^6$  CFU/mL and incubated with compound to test its activity until 20 passages had been reached. As shown in **Figure 6**, the MIC values of compound **2** were almost unchanged even after 20 passages, while that of norfloxacin increased 10-fold. This result demonstrated that **2** had minimum propensity to induce bacterial resistance.

### Inhibition of Biofilm

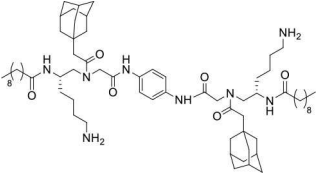
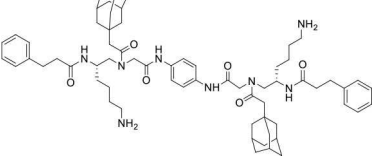
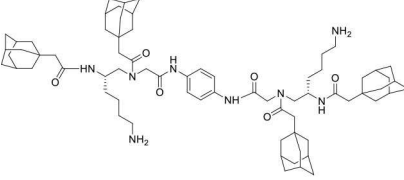
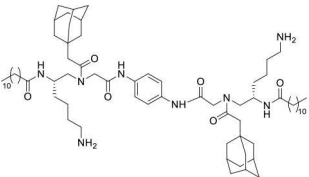
Biofilms, which have been increasingly recognized as a main accessory of drug resistance, is a community of bacteria living in cellular cluster or microcolonies encapsulated in a matrix consisted of extracellular polymers (Davies, 2003). Bacteria in

**TABLE 1** | Structures, MICs, and HC<sub>50</sub> of compound 1-14<sup>a</sup>.

#	Structure	MIC (μg/mL)			Hemolysis (HC <sub>50</sub> , μg/mL)	Selectivity index (HC <sub>50</sub> /MIC of MRSA)
		MRSA	MRSE	VRE		
1		2	<0.75	>25	>250	>125
2		2	1	10	250	125
3		2	1	20	250	>125
4		>25	>25	>25	>250	-
5		>25	>25	>25	>250	-
6		20	>25	>25	>250	>12.5
7		10	2	20	250	25
8		>25	>25	>25	250	-
9		2	10	>25	>250	>125
10		5	1	20	>250	>50

(Continued)

TABLE 1 | Continued

#	Structure	MIC ( $\mu\text{g/mL}$ )			Hemolysis ( $\text{HC}_{50}$ , $\mu\text{g/mL}$ )	Selectivity index ( $\text{HC}_{50}/\text{MIC}$ of MRSA)
		MRSA	MRSE	VRE		
11		>25	>25	>25	>250	-
12		5	2	10	125	25
13		5	2	20	250	50
14		>25	>25	>25	>250	-

<sup>a</sup>Bacteria included in the test were methicillin-resistant *S. aureus* (MRSA) (ATCC 33591), methicillin-resistant *S. epidermidis* (MRSE) (RP62A), and vancomycin-resistant *E. faecalis* (ATCC 700802). The most potent compound **2** is shown in red. The experiments were repeated three times.

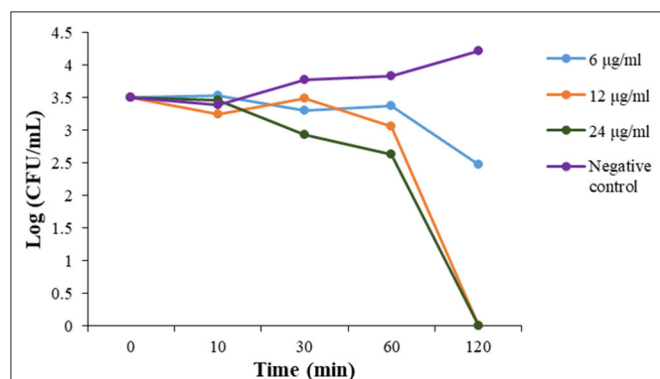


**FIGURE 2** | Time-kill kinetics of **2** against MRSA. The experiments were repeated three times.

biofilm are 10- to 1,000-fold more resistance to antibacterial agents (Hoque et al., 2015). Therefore, it is very significant to develop antibiotics with potency not only to inhibit the growth of biofilm, but also to eradicate the formed biofilm. Herein, one of our best compounds, **2**, was evaluated the eradication of established MRSA biofilm. As shown in **Figure 7**, at a

concentration of 0.06  $\mu\text{g/mL}$ , 55% biofilm can be inhibited by compound **2**. This result indicated the effectiveness of compound **2** as an antibacterial agent and was consistent with its satisfactory anti-drug resistance activity.

## CONCLUSION

In summary, a series of novel dimerized  $\gamma$ -AApeptide antibacterial compounds, mimicking HDPs, were rationally designed and synthesized. Most of these compounds showed excellent bacteria-killing efficacy against a panel of medically relevant multidrug resistant Gram-positive bacteria including MRSA, MRSE, and VRE. Notably, these compounds also exhibited high specificity toward bacteria, suggesting they are safe and promising agents to be applied for clinical use. Mechanism studies of the most potent compound **2** demonstrated that the compounds kill bacteria rapidly by interrupting membrane integrity, a way analogous to HDPs. Furthermore, compound **2** did not induce drug resistance, augmenting its therapeutic potential. Together with their small size and straightforward synthesis, the dimerized  $\gamma$ -AApeptides could be developed into a new generation of potential antibacterial agents to combat drug resistance.

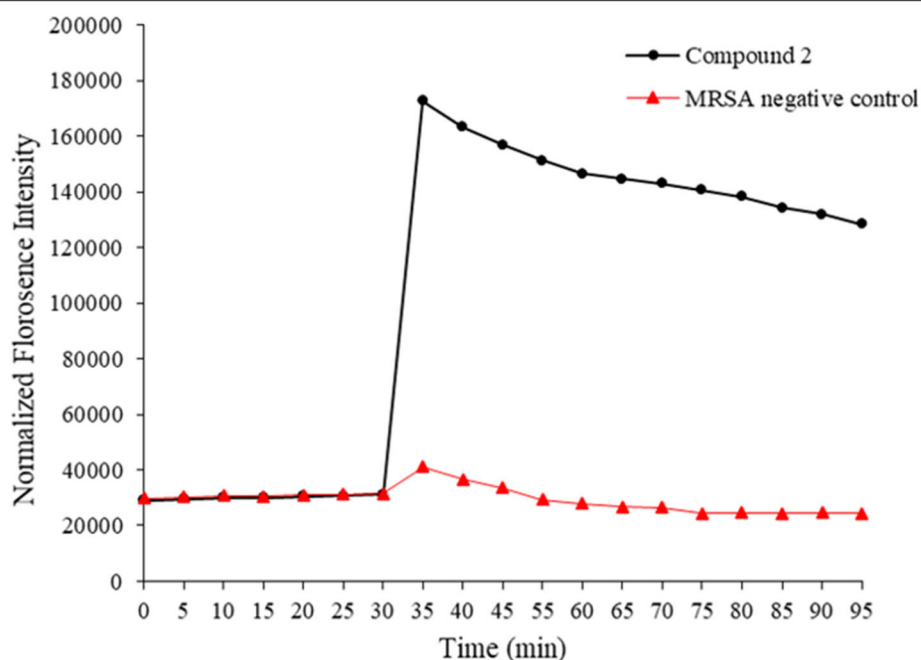


**FIGURE 3** | Membrane depolarization against MRSA. Negative control is bacteria without treatment of antibacterial agents. The experiments were repeated three times.

## EXPERIMENTAL SECTION

### General Information

All chemicals and solvent were purchased from either Sigma-Aldrich or Fisher Scientific and were used without further purification. All reactions were monitored by thin layer chromatography. Column chromatography was carried out with silica gel (200–300 mesh). Visualization was accomplished by using a UV (254 nm) lamp. The final products were purified on a Waters Breeze 2 HPLC system and lyophilized on a Labconco lyophilizer. The purity of the compounds was determined to be >95% by analytical HPLC [1 mL/min flow, 5–100% linear gradient of solvent B (0.1% TFA in acetonitrile) in A (0.1% TFA in water) over 40 min was used (detection wavelength was 215 nm or 254 nm). High resolution mass spectra of compounds were identified by an Agilent Technologies 6540 UHD accurate-mass Q-TOF LC/MS spectrometer. TEM images were obtained on a FEI Morgagni 268D TEM with an Olympus MegaView III camera on the microscope.

### Synthesis and Characterization

#### **N,N'-(((1,4-phenylenebis(2-oxoethane-2,1-diyl)) bis ((2-((3*r*,5*r*,7*r*)-adamantan-1-yl) acetyl) azanediy)) bis (6-aminohexane-1,2-diyl)) bis (decanamide) (11)**

The synthesis of other compounds is similar to **11**. The synthesis of structure **a** followed the method reported before (Teng et al., 2016b). 2-((3*r*,5*r*,7*r*)-adamantan-1-yl)acetyl chloride (625  $\mu$ L, 2.94 mmol) was added dropwise into the DCM (20 mL) solution of **a** (500 mg, 0.98 mmol) and diisopropylethylamine (DIPEA) (512  $\mu$ L, 2.94 mmol). After stirring for 2 h at room

temperature, the solution was diluted with 10 mL DCM and then washed with 1 M HCl (15 mL  $\times$  1), brine (15 mL  $\times$  1), and then dried with  $\text{Na}_2\text{SO}_4$  to afford crude **b**. After the solvent was removed under reduced pressure, the residue was purified by column chromatography on silica gel (petroleum ether: ethyl acetate = 1:1) to afford the pure product **b** (619 mg, 92%). 1-[Bis(dimethylamino)methylene]-1*H*-1,2,3-triazolo[4,5-*b*]pyridinium 3-oxid hexafluorophosphate (HATU) (441 mg, 1.16 mmol) was added to the DMF (20 mL) solution of 200 mg (0.29 mmol) **b**. Then, DIPEA (202  $\mu$ L, 1.16 mmol) was dropped into the above solution while stirring. At last, benzene-1,4-diamine (15.6 mg, 0.15 mmol) was added into the solution. After 2 h, the mixture was diluted with ethyl acetate 50 mL and then washed with 15 mL 1 M HCl, 50 mL  $\times$  3 brine.  $\text{Na}_2\text{SO}_4$  was applied to dry the solution. After being concentrated by rotavapor, crude **c** (169 mg, 83%) was obtained and used without further purification.  $\text{CH}_3\text{CN}$ :ethylenediamine = 1:1 solution was added to **c** to stir 30 min. After the solution was removed, cold ether was used to precipitate the crude product and the residue was blown to dry. Decanoyl chloride (91  $\mu$ L, 0.48 mmol) was dropped into the  $\text{CH}_2\text{Cl}_2$  (20 mL) solution with the crude product obtained from last step and DIPEA (84  $\mu$ L, 2.3 mmol). After stirring for 2 h, the solution was washed with 1 M HCl (15 mL  $\times$  1) and brine and dried with  $\text{Na}_2\text{SO}_4$  to afford crude **d**. Then, after evaporating the solution without any purification,  $\text{CH}_2\text{Cl}_2$ :trifluoroacetic acid = 1:1 was added into a flask with **c**, stirring at room temperature for 1 h. The whole solution was removed by rotavapor after the reactant had been completely consumed. Crude final product **11** was dissolved by  $\text{CH}_3\text{CN}$ : $\text{H}_2\text{O}$  = 2:1 and then purified by HPLC to obtain the pure compound

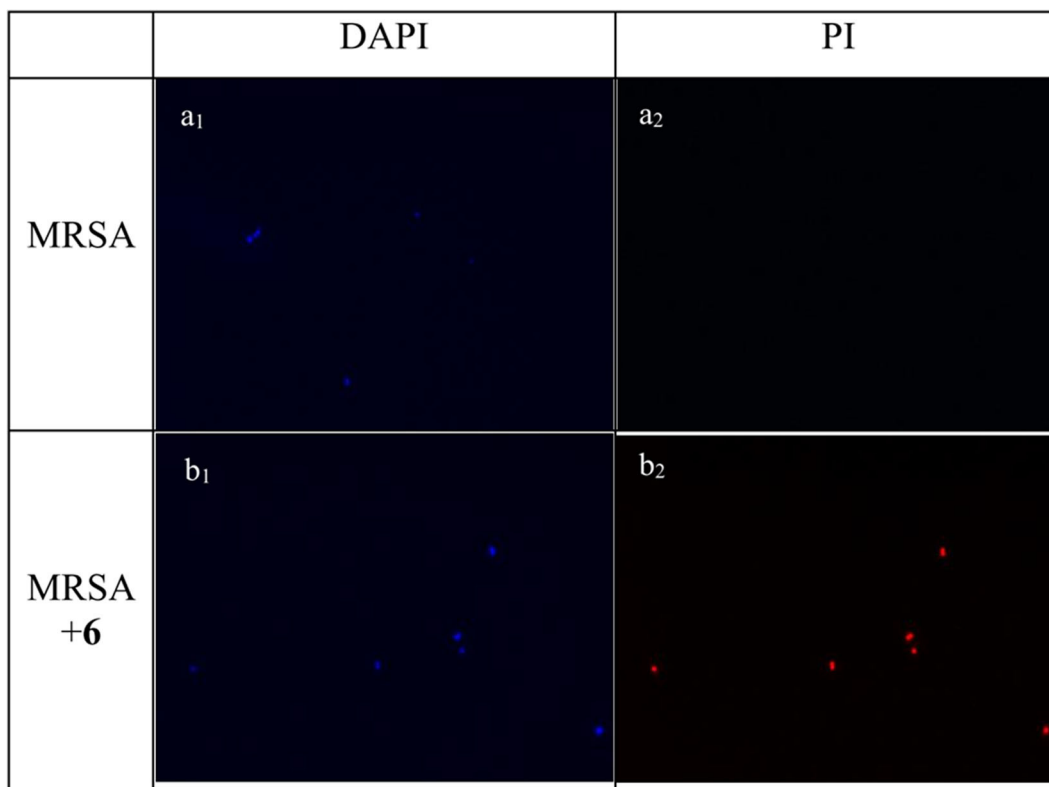


**FIGURE 4** | Fluorescence micrographs of MRSA in DAPI and PI channels. Bacteria was observed under 40 folds lens. **(a<sub>1</sub>)** Control, no treatment, DAPI channel. **(a<sub>2</sub>)** Control, no treatment, PI channel. **(b<sub>1</sub>)** MRSA treated with compound **2**, DAPI channel. **(b<sub>2</sub>)** MRSA treated with compound **2**, PI channel. The experiments were repeated three times.

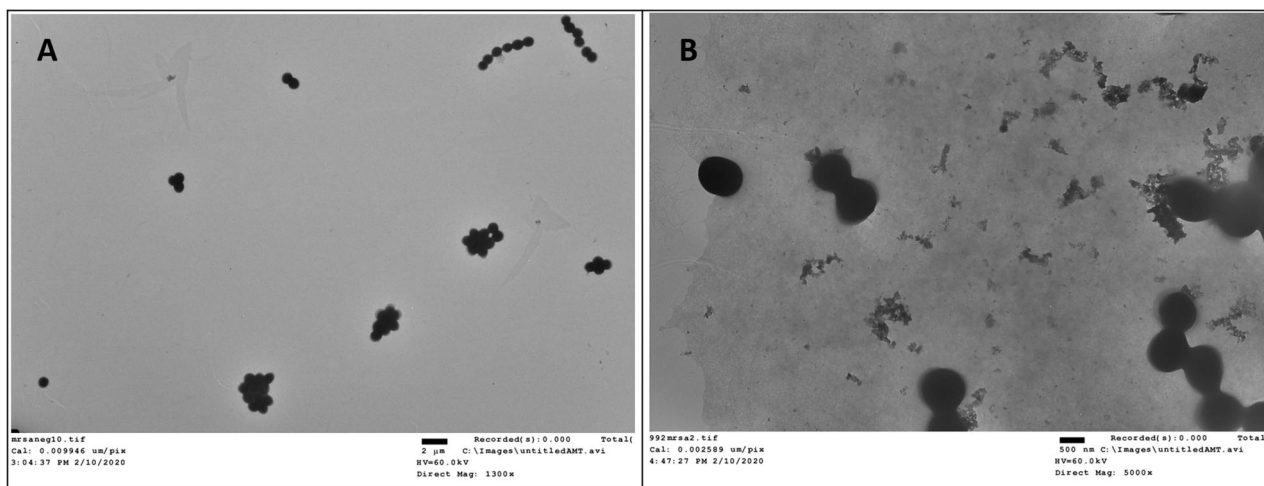


**FIGURE 5** | TEM study of compound **2** against MRSA. **(A)** Control, no treatment. **(B)** MRSA treated with compound **2**. The experiments were repeated three times.

**11** (26 mg, 20%) as a white solid. HRMS (ESI-TOF)  $m/z$   $C_{52}H_{82}O_8N_6$   $[M+H]^+$  calcd= 1111.8627; found= 1111.8670.

For compounds **1–5** and **9–10**, after obtaining the intermediate **c**,  $CH_3CN$ :ethylenediamine = 1:1 and DCM:TFA = 1:1 was directly used to remove Fmoc protecting group and

Boc protecting group following the method introduced above. All trace and Q-tof spectrum information is included in **Support Information**.

$N,N'$ -((1,4-phenylenebis(azanediyl))bis(2-oxoethane-2,1-diyl))bis(N-(2,6-diaminohexyl) octanamide) (**1**) HRMS

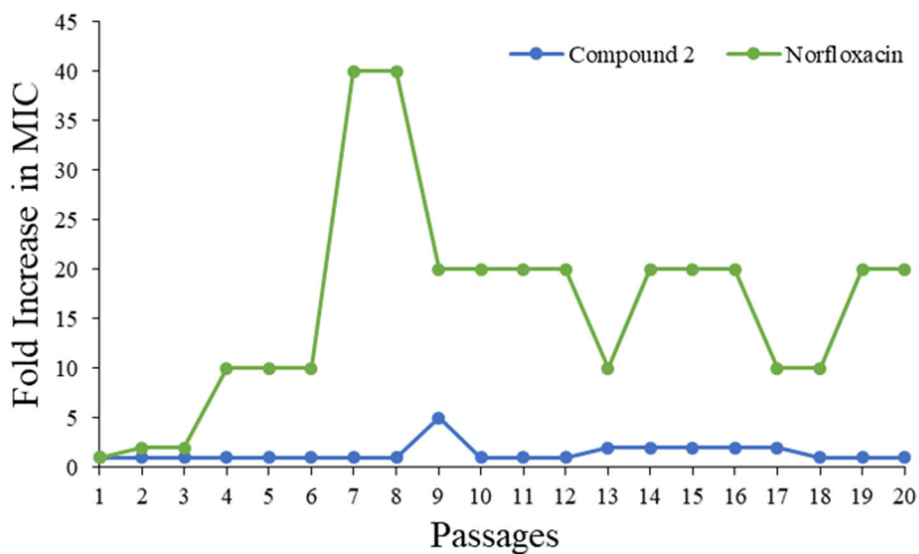


**FIGURE 6** | Drug resistance of compound **2** and Norfloxacin against MRSA.

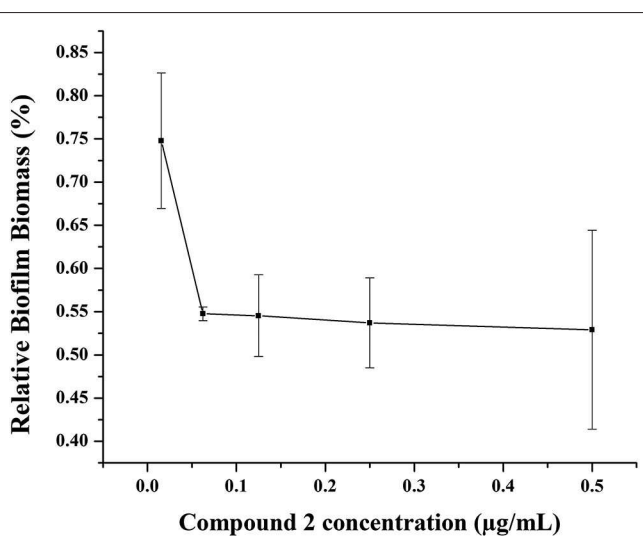


**FIGURE 7** | Biofilm disruption of compound **2**.

(ESI-TOF)  $m/z$   $C_{38}H_{70}O_8N_4$   $[M+H]^+$  calcd = 703.5598; found = 703.5592.

$N,N'$ -((1,4-phenylenebis(azanediyl))bis(2-oxoethane-2,1-diyl))bis(N-(2,6-diaminohexyl) decanamide) (**2**) HRMS (ESI-TOF)  $m/z$   $C_{42}H_{78}O_8N_4$   $[M+H]^+$  calcd = 759.6224; found = 759.6243.

$N,N'$ -((1,4-phenylenebis(azanediyl)) bis (2-oxoethane-2,1-diyl)) bis (N-(2,6-diaminohexyl) dodecanamide) (**3**) HRMS (ESI-TOF)  $m/z$   $C_{46}H_{86}O_8N_4$   $[M+H]^+$  calcd = 815.6850; found = 815.6880.

$N,N'$ -((1,4-phenylenebis(azanediyl))bis(2-oxoethane-2,1-diyl))bis(N-(2,6-diaminohexyl) tetradecanamide) (**4**) HRMS

(MALDI-TOF)  $m/z$   $C_{50}H_{94}N_8O_4$   $[M+H]^+$  calcd = 871.7476; found = 871.9586.

$N,N'$ -(((1,4-phenylenebis(azanediyl))bis(2-oxoethane-2,1-diyl))bis(N-(2,6-diaminohexyl) palmitamide) (**5**) HRMS (MALDI-TOF)  $m/z$   $C_{54}H_{103}N_8O_4$   $[M+H]^+$  calcd = 928.4700; found = 928.1901.

$N,N'$ -(((1,4-phenylenebis(azanediyl))bis(2-oxoethane-2,1-diyl)) bis (decanoylazanediy)) bis(6-aminoheptane-1,2-diyl))bis(2-naphthamide) (**6**) HRMS (ESI-TOF)  $m/z$   $C_{64}H_{90}O_8N_6$   $[M+H]^+$  calcd = 1,067.7062; found = 1,067.7017.

$N$ -(2-(2-(((1*s*,3*s*)-adamantan-1-yl)acetamido)-6-aminoheptyl)-N-(2-(((4-(2-(N-(2-(2-(((3*r*,5*r*,7*r*)-adamantan-1-yl)acetamido)-6-aminoheptyl) decanamido) acetamido) phenyl) amin)-2-oxoethyl)decanamide) (**7**) HRMS (ESI-TOF)  $m/z$   $C_{62}H_{103}O_8N_6$   $[M+H]^+$  calcd = 1,055.8001; found = 1,055.7969.

$N,N'$ -(((1,4-phenylenebis(azanediyl))bis(2-oxoethane-2,1-diyl))bis(octanoylazanediy)) bis(6-aminoheptane-1,2-diyl))bis(decanamide) (**8**) HRMS (ESI-TOF)  $m/z$   $C_{58}H_{106}O_8N_6$   $[M+H]^+$  calcd = 1,011.8314; found = 1,011.8356.

$N,N'$ -((1,4-phenylenebis(azanediyl))bis(2-oxoethane-2,1-diyl))bis(N-(2,6-diaminohexyl)-2-naphthamide) (**9**) HRMS (ESI-TOF)  $m/z$   $C_{44}H_{54}O_8N_4$   $[M+H]^+$  calcd = 759.4346; found = 759.4323.

$N,N'$ -((1,4-phenylenebis(azanediyl))bis(2-oxoethane-2,1-diyl))bis(2-(((3*r*,5*r*,7*r*)-adamantan-1-yl)-N-(2,6-diaminohexyl) acetamide) (**10**) HRMS (ESI-TOF)  $m/z$   $C_{46}H_{74}O_8N_4$   $[M+H]^+$  calcd = 803.5911; found = 803.5888.

$N,N'$ -(((1,4-phenylenebis(azanediyl))bis(2-oxoethane-2,1-diyl)) bis ((2-(((3*r*,5*r*,7*r*)-adamantan-1-yl)acetyl)azanediyl))bis(6-aminoheptane-1,2-diyl))bis(decanamide) (**11**) HRMS (ESI-TOF)  $m/z$   $C_{66}H_{110}N_8O_6$   $[M+H]^+$  = 1,111.8627; found = 1,111.8670.

$N,N'$ -(((1,4-phenylenebis(azanediyl)) bis (2-oxoethane-2,1-diyl)) bis ((2-(((3*r*,5*r*,7*r*)-adamantan-1-yl)acetyl)azanediyl))bis(6-aminoheptane-1,2-diyl)) bis (3-phenylpropanamide) (**12**) HRMS



(ESI-TOF)  $m/z$   $C_{64}H_{90}O_8N_6$   $[M+H]^+$  calcd = 1,067.7064; found = 1,067.7030.

$N,N'$ -(((1,4-phenylenebis(azanediyl))bis(2-oxoethane-2,1-diyl))bis(2-((3*r*,5*r*,7*r*)-adamantan-1-yl)-N-(2-(2-((3*r*,5*r*,7*r*)-adamantan-1-yl)acetamido)-6-aminoethyl)acetamide) (13) HRMS (ESI-TOF)  $m/z$   $C_{58}H_{106}O_8N_6$   $[M+H]^+$  calcd = 1,155.8314; found = 1,155.8282.

$N,N'$ -(((1,4-phenylenebis(azanediyl))bis(2-oxoethane-2,1-diyl))bis(2-((3*r*,5*r*,7*r*)-adamantan-1-yl)acetylazanediyl))bis(6-aminohexane-1,2-diyl)didodecanamide (14) HRMS (ESI-TOF)  $m/z$   $C_{58}H_{106}O_8N_6$   $[M+H]^+$  calcd = 1,167.9253; found = 1,167.9215.

## Minimum Inhibitory Concentrations (MICs) against Bacteria

The antimicrobial assay of the compounds was conducted on the following three bacteria strains: *methicillin-resistant S. aureus* (MRSA, ATCC 33591), *methicillin-resistant S. epidermidis* (MRSE, RP62A), and *vancomycin-resistant E. faecalis* (VRE, ATCC 700802). The procedures were followed as reported previously. (Isaksson et al., 2011) The MICs were determined as the lowest concentration that completely inhibits the bacteria growth. All measurements were repeated at least three times with duplicates each time.

## Hemolysis Study

Fresh red blood cell (RBC) of mice was collected by centrifuge with the speed of 500 *g* for 10 mins until the supernatant is clear. Then, the RBC was diluted with PBS for 20-fold. After adding 50  $\mu$ L PBS in each vial on 96 plates, 1 mg/mL compounds were serially diluted until reaching the lowest concentration 1.9  $\mu$ g/mL. Diluted RBC was added into each vial and incubated at 37°C for 1 h. Then, plates were centrifuged at 2,301 *g* (3,500 rpm) for 10 mins. 30  $\mu$ L supernatant in each vial was added into 100  $\mu$ L PBS and read Biotek Synergy HT plate reader at 540 nm. The hemolytic activity was calculated by the formula % hemolysis = (Abs<sub>sample</sub> - Abs<sub>PBS</sub>) / (Abs<sub>Triton</sub> - Abs<sub>PBS</sub>)  $\times$  100%. 1% Triton X-100 were used as the positive control and 1  $\times$  PBS buffer was used as the negative control.

## Time-Kill Study

Time-kill kinetic study of compound 2 were investigated. After being incubated from one colony in 4 mL TSB medium overnight at 37 °C while shaking, MRSA was diluted 2,500 times to another fresh 4 mL TSB solution and grew for 6~8 h to mid-logarithmic phase. Suspension [ $10^6$  colony-forming units per milliliter (CFU/mL) according to the read of OD value] was made and then incubated with different concentration of 2 at 37°C for 10 min, 30 min, 60 min, 120 min respectively. The MRSA and drug mixture were diluted  $10^2$ -fold and spread on the TSB agar plates. These plates were incubated at 37°C overnight. The numbers of colonies on each plate were transferred to lg[CFU/mL] and plotted against the incubation time. The experiment was repeated three times with duplicates each time.

## Fluorescence Microscopy

Fluorescent dyes propidium iodide (PI) and 4',6'-diamidino-2-phenylindole dihydrochloride (DAPI) can be used to distinguish the viable cell from the dead cells. After obtaining the mid-logarithmic phase bacteria solution as above, the bacteria solution was diluted 100 times and mixed with compound 2 at the concentration of 6  $\mu$ g/mL. Then the mixture was incubated 2 h and centrifuged at 1,690 *g* (3,000 rpm) for 15 min at 4°C to harvest the cells. After washing with PBS for 3 times, PI (5  $\mu$ g/mL) and DAPI (10  $\mu$ g/mL) was used to dye cells 20 min respectively. Controls were carried out without compounds. The bacterial cells were then visualized and analyzed by employing the LEICA DM 2000 optical microscope with an oil-immersion objective (40 $\times$ ). The experiment was repeated three times with duplicates each time.

## Membrane Depolarization Study

Mid log phase MRSA bacteria solution was obtained as above. Then, cells were collected and washed with 5 mM HEPES and 5 mM glucose respectively. 5 mM HEPES:5 mM glucose:100 mM KCl = 1:1:1 was used to resuspended bacteria cells ( $10^6$  CFU/mL). Following that, 200  $\mu$ L of bacterial suspension and 1  $\mu$ M DiSC3(5) were included in a 96-well plate, and the fluorescence of the suspension was monitored at room temperature for 30 min at excitation wavelength of 622 nm and emission wavelength of 670 nm. After 30 min, compound 2 was added to the wells and the increased potential was monitored. The experiment was repeated three times with duplicates each time.

## Drug Resistance Study

The experiment was carried out by following our previously reported protocol (Su et al., 2017; Niu et al., 2018). The study was conducted for 20 passages.

## TEM Study

After being incubated to mid log phase, MRSA ( $10^6$  CFU/mL) was mixed with 6  $\mu$ g/mL compound 2 for 2 h. Then the bacteria cells were collected and washed with PBS and DI water. Following that, bacteria was resuspended in deionized water. Control bacterial samples were obtained without adding drugs. Above samples were applied to TEM grids by 5  $\mu$ L bacteria solution, and the grids were allowed to dry in vacuum oven at the temperature of 45°C for 45 seconds. After being dried, TEM images were obtained on a FEI Morgagni 268D TEM with an Olympus MegaView III camera at 60 kV on the microscope. The microscope used AnalySiS software to run the camera.

## Biofilm Inhibition Study

Incubating the compound 2 of different concentrations and suspended bacteria ( $10^6$  CFU/mL) in TSB (Tryptic soy broth) medium at 37°C for 48 h. Then, the 96-well plate was reversed and the suspending bacteria was discarded. After washing with DI water for several times, biofilm was dried in air at room temperature. Subsequently, 125  $\mu$ L 0.1% crystal violet was added into all vials to dye for 15 mins. Extra dye was discarded and washed. Adding 200  $\mu$ L 30% acetic acid to dissolve colored

biofilm. Finally, 125  $\mu$ L acetic acid was transfer into another clean plate. OD values were read at 595 nm.

## DATA AVAILABILITY STATEMENT

The raw data supporting the conclusions of this article will be made available by the authors, without undue reservation, to any qualified researcher.

## ETHICS STATEMENT

The animal study was reviewed and approved by the ethics committee of the University of South Florida (protocol number R IS00005111).

## AUTHOR CONTRIBUTIONS

All authors listed made a substantial, direct and intellectual contribution to the work. MW synthesized all the compounds and conducted all the antibacterial assays. RG evaluated the

hemolytic assay. PS provided valuable advice for compounds design. TO corrected the grammar mistakes and typos in this article, and he also helped with the experimental design and did the HPLC trace analysis. MZ finished the Q-tof spectrum test. YS provided suggestions on synthesis. HX provided methods on antibacterial assays. CC provided biolevel II lab and mice blood. JC designed all structures and provided funding.

## FUNDING

This work was supported by NHI R01AI149852, NHI R01AI152416, and NSF1708500.

## SUPPLEMENTARY MATERIAL

The Supplementary Material for this article can be found online at: <https://www.frontiersin.org/articles/10.3389/fchem.2020.00441/full#supplementary-material>

## REFERENCES

- Becker, K., Herold-Mende, C., Park, J. J., Lowe, G., and Schirmer, R. H. (2001). Human thioredoxin reductase is efficiently inhibited by (2,2':6;2'-terpyridine)platinum(II) complexes. *Possible implications for a novel antitumor strategy*. *J. Med. Chem.* 44, 2784–2792. doi: 10.1021/jm001014i
- Chongsiriwatana, N. P., Miller, T. M., Wetzler, M., Vakulenko, S., Karlsson, A. J., Palecek, S. P., et al. (2011). Short alkylated peptoid mimics of antimicrobial lipopeptides. *Antimicrob. Agents Chemother.* 55, 417–420. doi: 10.1128/AAC.01080-10
- Chongsiriwatana, N. P., Patch, J. A., Czyzewski, A. M., Dohm, M. T., Ivankin, A., Gidalevitz, D., et al. (2008). Peptides that mimic the structure, function, and mechanism of helical antimicrobial peptides. *Proc. Natl. Acad. Sci. U. S. A.* 105, 2794–2799. doi: 10.1073/pnas.0708254105
- Davies, D. (2003). Understanding biofilm resistance to antibacterial agents. *Nat. Rev. Drug Discov.* 2, 114–122. doi: 10.1038/nrd1008
- Debnath, B., Xu, S., and Neamati, N. (2012). Small molecule inhibitors of signal transducer and activator of transcription 3 (Stat3) protein. *J. Med. Chem.* 55, 6645–6668. doi: 10.1021/jm300207s
- Galdiero, E., Siciliano, A., Maselli, V., Gesuele, R., Guida, M., Fulgione, D., et al. (2016). An integrated study on antimicrobial activity and ecotoxicity of quantum dots and quantum dots coated with the antimicrobial peptide indolicidin. *Int. J. Nanomed.* 11, 4199–4211. doi: 10.2147/IJN.S107752
- Ghosh, A. K., and Brindisi, M. (2015). Organic carbamates in drug design and medicinal chemistry. *J. Med. Chem.* 58, 2895–2940. doi: 10.1021/jm501371s
- Hoque, J., Konai, M. M., Gonuguntla, S., Manjunath, G. B., Samaddar, S., Yarlagadda, V., et al. (2015). Membrane active small molecules show selective broad spectrum antibacterial activity with no detectable resistance and eradicate biofilms. *J. Med. Chem.* 58, 5486–5500. doi: 10.1021/acs.jmedchem.5b00443
- Hu, Y., Amin, M. N., Padhee, S., Wang, R. E., Qiao, Q., Bai, G., et al. (2012). Lipidated peptidomimetics with improved antimicrobial activity. *ACS Med. Chem. Lett.* 3, 683–686. doi: 10.1021/ml3001215
- Hua, J., Scott, R. W., and Diamond, G. (2010). Activity of antimicrobial peptide mimetics in the oral cavity: II. Activity against periopathogenic biofilms and anti-inflammatory activity. *Mol. Oral Microbiol.* 25, 426–432. doi: 10.1111/j.2041-1014.2010.00591.x
- Isaksson, J., Brandsdal, B. O., Engqvist, M., Flaten, G. E., Svendsen, J. S. M., and Stensen, W. (2011). A synthetic antimicrobial peptidomimetic (LTX 109): stereochemical impact on membrane disruption. *J. Med. Chem.* 54, 5786–5795. doi: 10.1021/jm200450h
- Karlsson, A. J., Flessner, R. M., Gellman, S. H., Lynn, D. M., and Palecek, S. P. (2010). Polyelectrolyte multilayers fabricated from antifungal  $\beta$ -peptides: design of surfaces that exhibit antifungal activity against candida albicans. *Biomacromolecules* 11, 2321–2328. doi: 10.1021/bm100424s
- Karlsson, A. J., Pomerantz, W. C., Weisblum, B., Gellman, S. H., and Palecek, S. P. (2006). Antifungal activity from 14-helical  $\beta$ -peptides. *J. Am. Chem. Soc.* 128, 12630–12631. doi: 10.1021/ja064630y
- Lee, A. S., de Lencastre, H., Garau, J., Kluytmans, J., Malhotra-Kumar, S., Peschel, A., et al. (2018). Methicillin-resistant *Staphylococcus aureus*. *Nat. Rev. Dis. Primers* 4:18033. doi: 10.1038/nrdp.2018.33
- Lei, R., Hou, J., Chen, Q., Yuan, W., Cheng, B., Sun, Y., et al. (2018). Self-assembling myristoylated human  $\alpha$ -defensin 5 as a next-generation nanobiotics potentiates therapeutic efficacy in bacterial infection. *ACS Nano* 12, 5284–5296. doi: 10.1021/acsnano.7b09109
- Li, C., Teng, P., Peng, Z., Sang, P., Sun, X., and Cai, J. (2018). Bis-cyclic guanidines as a novel class of compounds potent against clostridium difficile. *ChemMedChem* 13, 1414–1420. doi: 10.1002/cmdc.201800240
- Li, Y., Smith, C., Wu, H., Padhee, S., Manoj, N., Cardillo, J., et al. (2014a). Lipidated cyclic  $\gamma$ -Aapeptides display both antimicrobial and anti-inflammatory activity. *ACS Chem. Biol.* 9, 211–217. doi: 10.1021/cb4006613
- Li, Y., Smith, C., Wu, H., Teng, P., Shi, Y., Padhee, S., et al. (2014b). Short antimicrobial lipo- $\alpha$ / $\gamma$ -AA hybrid peptides. *ChemBioChem* 15, 2275–2280. doi: 10.1002/cbic.201402264
- Méndez-Samperio, P. (2014). Peptidomimetics as a new generation of antimicrobial agents: current progress. *Infect. Drug Resist.* 7, 229–237. doi: 10.2147/IDR.S49229
- Molchanova, N., Hansen, P. R., and Franzyk, H. (2017). Advances in development of antimicrobial peptidomimetics as potential drugs. *Molecules* 22:1430. doi: 10.3390/molecules22091430
- Nimmagadda, A., Liu, X., Teng, P., Su, M., Li, Y., Qiao, Q., et al. (2017). Polycarbonates with potent and selective antimicrobial activity toward gram-positive bacteria. *Biomacromolecules* 18, 87–95. doi: 10.1021/acs.biomac.6b01385
- Niu, Y., Wang, M., Cao, Y., Nimmagadda, A., Hu, J., Wu, Y., et al. (2018). Rational design of dimeric lysine N-alkylamides as potent and broad-spectrum antibacterial agents. *J. Med. Chem.* 61, 2865–2874. doi: 10.1021/acs.jmedchem.7b01704
- Padhee, S., Li, Y., and Cai, J. (2015). Activity of lipo-cyclic  $\gamma$ -Aapeptides against biofilms of *Staphylococcus epidermidis* and *Pseudomonas aeruginosa*. *Bioorg. Med. Chem. Lett.* 25, 2565–2569. doi: 10.1016/j.bmcl.2015.04.039

- Payne, D. J., Gwynn, M. N., Holmes, D. J., and Pompliano, D. L. (2006). Drugs for bad bugs: confronting the challenges of antibacterial discovery. *Nat. Rev. Drug Discov.* 6, 29–40. doi: 10.1038/nrd2201
- Rotem, S., Raz, N., Kashi, Y., and Mor, A. (2010). Bacterial capture by peptide-mimetic oligoacetylsine surfaces. *Appl. Environ. Microbiol.* 76, 3301–3307. doi: 10.1128/AEM.00532-10
- She, F., Teng, P., Peguero-Tejada, A., Wang, M., Ma, N., Odom, T., et al. (2018). *De novo* left-handed synthetic peptidomimetic foldamers. *Angew. Chem.* 57, 9916–9920. doi: 10.1002/anie.201805184
- Shi, C., Zhang, Y., Wang, T., Lu, W., Zhang, S., Guo, B., et al. (2019a). Design, synthesis, and biological evaluation of novel DNA gyrase-inhibiting spiropyrimidinetriones as potent antibiotics for treatment of infections caused by multidrug-resistant gram-positive bacteria. *J. Med. Chem.* 62, 2950–2973. doi: 10.1021/acs.jmedchem.8b01750
- Shi, Y., Teng, P., Sang, P., She, F., Wei, L., and Cai, J. (2016).  $\gamma$ -AApeptides: design, structure, and applications. *Acc. Chem. Res.* 49, 428–441. doi: 10.1021/acs.accounts.5b00492
- Shi, Y., Yin, G., Yan, Z., Sang, P., Wang, M., Brzozowski, R., et al. (2019b). Helical sulfono- $\gamma$ -AApeptides with aggregation-induced emission and circularly polarized luminescence. *J. Am. Chem. Soc.* 141, 12697–12706. doi: 10.1021/jacs.9b05329
- Singh, S., Nimmagadda, A., Su, M., Wang, M., Teng, P., and Cai, J. (2018). Lipidated  $\alpha/\alpha$ -AA heterogeneous peptides as antimicrobial agents. *Eur. J. Med. Chem.* 155, 398–405. doi: 10.1016/j.ejmech.2018.06.006
- Su, M., Xia, D., Teng, P., Nimmagadda, A., Zhang, C., Odom, T., et al. (2017). Membrane-active hydantoin derivatives as antibiotic agents. *J. Med. Chem.* 60, 8456–8465. doi: 10.1021/acs.jmedchem.7b00847
- Teng, P., Gray, G. M., Zheng, M., Singh, S., Li, X., Wojtas, L., et al. (2019). Orthogonal halogen-bonding-driven 3D supramolecular assembly of right-handed synthetic helical peptides. *Angew. Chem.* 58, 7778–7782. doi: 10.1002/anie.201903259
- Teng, P., Huo, D., Nimmagadda, A., Wu, J., She, F., Su, M., et al. (2016a). Small antimicrobial agents based on acylated reduced amide scaffold. *J. Med. Chem.* 59, 7877–7887. doi: 10.1021/acs.jmedchem.6b00640
- Teng, P., Ma, N., Cerrato, D. C., She, F., Odom, T., Wang, X., et al. (2017a). Right-handed helical foldamers consisting of *de novo* d-AApeptides. *J. Am. Chem. Soc.* 139, 7363–7369. doi: 10.1021/jacs.7b03007
- Teng, P., Nimmagadda, A., Su, M., Hong, Y., Shen, N., Li, C., et al. (2017b). Novel bis-cyclic guanidines as potent membrane-active antibacterial agents with therapeutic potential. *ChemComm* 53, 11948–11951. doi: 10.1039/C7CC07285F
- Teng, P., Niu, Z., She, F., Zhou, M., Sang, P., Gray, G. M., et al. (2018). Hydrogen-bonding-driven 3D supramolecular assembly of peptidomimetic zipper. *J. Am. Chem. Soc.* 140, 5661–5665. doi: 10.1021/jacs.7b11997
- Teng, P., Shi, Y., Sang, P., and Cai, J. (2016b).  $\gamma$ -AApeptides as a new class of peptidomimetics. *Chem. Eur. J.* 22, 5458–5466. doi: 10.1002/chem.201504936
- Teyssières, E., Corre, J.-P., Antunes, S., Rougeot, C., Dugave, C., Jouvion, G., et al. (2016). Proteolytically stable foldamer mimics of host-defense peptides with protective activities in a murine model of bacterial infection. *J. Med. Chem.* 59, 8221–8232. doi: 10.1021/acs.jmedchem.6b00144
- Wang, T. Z., Kodyanplakkal, R. P. L., and Calfee, D. P. (2019). Antimicrobial resistance in nephrology. *Nat. Rev. Nephrol.* 15, 463–481. doi: 10.1038/s41581-019-0150-7
- Wu, H., Niu, Y., Padhee, S., Wang, R. E., Li, Y., Qiao, Q., et al. (2012). Design and synthesis of unprecedented cyclic  $\gamma$ -AApeptides for antimicrobial development. *Chem. Sci.* 3, 2570–2575. doi: 10.1039/c2sc20428b

**Conflict of Interest:** The authors declare that the research was conducted in the absence of any commercial or financial relationships that could be construed as a potential conflict of interest.

Copyright © 2020 Wang, Gao, Sang, Odom, Zheng, Shi, Xu, Cao and Cai. This is an open-access article distributed under the terms of the Creative Commons Attribution License (CC BY). The use, distribution or reproduction in other forums is permitted, provided the original author(s) and the copyright owner(s) are credited and that the original publication in this journal is cited, in accordance with accepted academic practice. No use, distribution or reproduction is permitted which does not comply with these terms.